Journal of Applied Polymer Science

Unique Pressure-Crystallized Structures in Ternary Bisphenol-A Polycarbonate/Dioctyl Phthalate/Fullerene C60 Composites

Jiaojiao Tian,[1] Guodong Liu,[1] Xin Chen,[1] Jun Lu,[1] Zuowan Zhou,[1] Rui Huang[2]

[1]Key Laboratory of Advanced Technologies of Materials, Ministry of Education, School of Materials Science and Engineering, Southwest Jiaotong University, Chengdu 610031, Sichuan, China

[2]College of Polymer Materials Science and Engineering, Sichuan University, Chengdu 610065, Sichuan, China

Correspondence to: J. Lu (E-mail: junluprc@hotmail.com)

ABSTRACT: We report pressure-controlled fast growth of unique crystalline structures of bisphenol-A polycarbonate (PC) was achieved by the introduction of both dioctyl phthalate (DOP) and fullerene C60. PC/DOP/C60 ternary composites with an overall good C60 dispersion were prepared by an easy physical and mechanical route, and then crystallized in a piston-cylinder high-pressure apparatus by varying temperature, pressure, crystallization time and composite composition. The crystallization of PC was greatly hastened by the blending with DOP and C60, and its melting point was increased to 288.25 degrees centigrade by the subsequent high-pressure treatment, which was around 40° centigrade higher than that of the samples crystallized at normal pressure. Three-dimensional spiky crystalline spheres were formed with the increase of crystallization temperature, which began with zero-dimensional nanogranules, and then developed by merging process through the stages of one-dimensional lamellar crystallites and two-dimensional dendrites. With pressure increased, the granules merged first into plate crystals, and then into micro-spheres with rugged surfaces or porous structures. Also, sometimes the granules organized into rugged crystalline nanoballs, and peony-like stereo-open structures were observed by changing composite composition. The as-prepared three-dimensional crystalline structures, with their large specific areas, may diversify niche functional applications as surface active materials. © 2012 Wiley Periodicals, Inc. J. Appl. Polym. Sci. 129: 1362–1373, 2013

KEYWORDS: composites; morphology; nanotubes; graphene and fullerenes; phase behavior; polycarbonates

Received 2 October 2012; accepted 12 November 2012; published online 7 December 2012
DOI: 10.1002/app.38822

INTRODUCTION

Polymer/fullerene composite is a very attractive field that integrates two expanding scientific areas, i.e., those of polymers and fullerenes.[1] The combination of fullerenes with polymers makes it possible to create novel materials that exhibit the unique properties of fullerenes while take advantages of the easy processability of polymers.[1,2] It has been shown that incorporating fullerene or its derivatives into a polymer matrix could significantly improve its photovoltaic, electromechanical, and thermomechanical properties.[3,4] However, compared with other carbon materials, such as carbon nanotubes, their outstanding mechanical, chemical, electrochemical, and photophysical properties still are not widely employed in polymers for real applications.[1]

As an engineering polymer of high performance, bisphenol-A polycarbonate (PC) is currently being employed in many aspects such as transportation, aerospace, construction, photonics, holographic data storage and other security applications, mainly due to its excellent toughness, weatherability, and transparency.[5–9] Although a wealth of studies has been published on the chemical synthesis and optical properties of fullerene-functionalized PC,[1,10–12] very few were addressed on the preparation of PC/fullerene nanocomposites by a physical process.

It is known that the crystallization behaviors of polymers have significant influence on their physical and mechanical properties. Especially, morphology control of polymer crystals is crucial in determining the final performance of polymeric functional devices.[13–18] As for PC, its bulk crystallization is extremely slow because of an inherent rigid nature of the molecular backbone.[19–21] So it is interesting to improve its crystallization ability so as to perform the crystalline morphology control of the polymer for functional applications. Several inorganic or organic nanofillers, such as multiwalled carbon nanotube (CNT) and clay, were already employed to improve the crystallization and other physical properties of PC.[22–24] Krause et al.[22] investigated the influence of dry grinding in a ball mill on the length of multiwalled carbon nanotubes and their dispersion and percolation

© 2012 Wiley Periodicals, Inc.

Table I. Characteristic Thermal Properties of the Starting PC/C60 and PC/DOP/C60 Composite Materials

Starting material	Composition (PC/DOP/C60, wt/wt/wt)	T_g (°C)	T_{cc} (°C)	ΔH_{cc} (J/g)	T_m (°C)	ΔH_m (J/g)
PC1	99.5/0.0/0.5	149.58	–	–	–	–
PC2	99.0/0.0/1.0	148.72	–	–	–	–
PC3	89.5/10.0/0.5	98.04	–	–	–	–
PC4	79.5/20.0/0.5	–	–	–	220.97	5.12
PC5	89.0/10.0/1.0	111.84	–	–	–	–
PC6	79.0/20.0/1.0	–	138.30	6.21	219.30	20.77

T_g, glass transition temperature; T_{cc}, cold crystallization temperature; ΔH_{cc}, enthalpy of cold crystallization; T_m, melting point; ΔH_m, melting enthalpy.

behavior in melt mixed PC composites. The slight increase in the electrical percolation threshold was observed in the melt mixed composites with ball milling time of CNTs, which was assigned to lower nanotube lengths as well as the worse dispersion of the ball-milled nanotubes. Two organic modified clays (CL30B and MB30B) were used to improve the mechanical properties of PC/poly (styrene-*co*-acrylonitrile) (SAN) blends by Lin et al.[23] Their results showed that dispersion of the clay platelets was better when MB30B was used. Also, the mechanical properties of the clay filled nanocomposites varied accordingly, and when MB30B was used better mechanical properties was achieved. Particularly, Münstedt[24] recently investigated the influence of crystallinity on rheological properties of unfilled and particle-filled PC. The research demonstrated that the crystallization of PC in the molten state had to be taken into account for a comprehensive assessment of rheological experiments, particularly evident in the case of filled particles acting as a nucleating agent. Nevertheless, to the best of our knowledge, no investigation was performed on PC crystallization by utilizing fullerenes at high pressure.

In this work, pressure-controlled fast growth of unique crystalline structures of PC was achieved for the first time by the simultaneous introduction of dioctyl phthalate (DOP), a viscous plasticizer, and fullerene C60. This strategy is based on the followings: it has been reported that the crystallization rate of polymers was increased by appropriate pressure treatment,[25,26] and the chain mobility of such aromatic polymer was hastened significantly simply through the incorporation of a viscous plasticizer.[27–30] In addition to serving as a nucleating agent to decrease the crystallization active energy in the ternary system, C60 was found recently to be a promising material in promoting the formation of new polymeric structures at high pressure.[31] By varying the temperature, pressure, crystallization time, and composition of the well-dispersed PC/DOP/C60 composites, which were fabricated via an easy physical and mechanical route, three-dimensional crystalline spheres with open structures and different characteristics, were finally grown from a zero-dimensional nanogranule by a merging process.

EXPERIMENTAL

Materials

PC in pellet form was a commercial product supplied by LG-DOW, Korea. The viscosity-average molecular weight, calculated from intrinsic viscosity, was about 11,000 g/mol. Analytical-grade DOP and dimethylacetamide, used as a plasticizer and an etchant, respectively, were provided by Kelong Chem, Chengdu, China. C60 powder (>99.9 wt/wt purity) was purchased from Puyang Yongxin Fullerene, and used as received. PC and C60 were premixed at 23,000 rpm for 10 min in a commercial blender (JYL-C012, Joyoung, China) with four stainless steel grinding blades. The unique intelligent temperature control system of the blender kept the mixture at room temperature during the pre-mixing process. This was followed by melt compounding at 30 rpm and 250°C for 15 min using a torque rheometer (ZJL-300, Changchun Intelligent Instrument Company, Changchun, China). The mixing structure was composed of the mixing chamber, rotor shafts, and transverse sealed device, which was fixed to the engine seat by support seats. Then the resultant PC/C60 mixtures and DOP, with a total weight of 50 g, were further melt-blended with the same process. This finally resulted in a sepia-colored composite material, which lost the transparency of the original PC. The as-prepared PC/DOP/C60 ternary composites were pelletized subsequently by using a smashing machine (FW400A, Beijing Zhongxingweiye Instrument, Beijing, China) for high-pressure experiments. No shear was involved during the smashing process. The compounding ratios of the starting materials are listed in Table I. Before melt blending and high-pressure treatment, the starting materials (PC, C60, PC/C60, and PC/DOP/C60 blends) were held at 95°C in vacuum for 24 h to eliminate moisture.

Sample Preparation

High-pressure experiments for the as-fabricated PC/DOP/C60 composites were carried out with a self-made piston-cylinder high-pressure apparatus. Its schematic drawing and the corresponding sample assembly are shown in Figure 1. The following procedure for crystallization was used. After loading the samples, low pressure (50 MPa) was applied, and then temperature was raised to a predetermined level. When equilibrium was established, the pressure was further raised to the predetermined level. These samples were kept under these conditions for a predetermined time, and then quenched down to ambient condition. This procedure ensured the minimum degradation of PC at elevated temperature, and the polymer would be in a molten state before crystallization took place. The crystallization conditions, including the crystallization temperature, pressure and time, are listed in Tables II–V.

Characterization

Transmission electron microscopy (TEM) was performed with a Tecnai G^2 F20 S-TWIN apparatus (FEI, USA), employing a

Applied Polymer SCIENCE

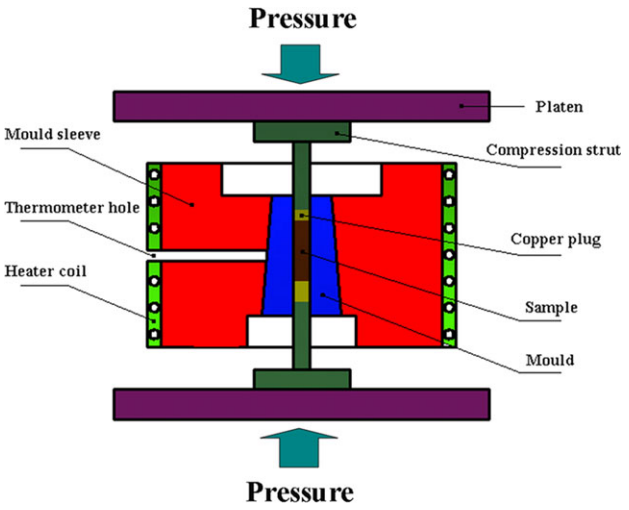

Figure 1. Schematic drawing of the employed piston-cylinder high-pressure apparatus and the corresponding sample assembly. [Color figure can be viewed in the online issue, which is available at wileyonlinelibrary.com.]

Leica EMUC6/FC6 microtome for the preparation of ultrathin sections through room-temperature microtomy. Wide-angle X-ray diffraction (WAXD) results were obtained at room temperature with a PANalytical X'pert PRO diffractometer (PANalytical BV, Almelo, the Netherlands).

Differential scanning calorimetry (DSC) was conducted at atmospheric pressure by using a TA-Q20 instrument (TA Instruments, USA). The weight of sample was around 5 mg. The melting behavior of the crystals was investigated through a heating scan with a heating rate of 10°C/min at N_2 atmosphere. The crystallinity X_c was calculated from the melting enthalpy ΔH_m by means of the following equation:[30]

$$X_c = \Delta H_m / \left(\Delta H_m^o \omega(\mathrm{PC})\right), \quad (1)$$

where ω (PC) is the weight ratio of PC in the blends, and $\Delta H_m{}^o$ is the melting enthalpy of the ideal crystal, which was assumed to be 109.7 J/g according to Legras et al.[29]

Scanning electron microscopy (SEM) was carried out on a HITACHI S-3400 apparatus (Hitachi, Tokyo, Japan). The fresh surfaces of the samples were obtained through fracture at liquid N_2 temperature, and then coated with gold for observation. Prior to the gold treatment, the surfaces were etched by dimethylacetamide at constant temperature for a given time, which is capable of dissolving only amorphous, but not crystalline PC.[32]

Table II. The Crystallization Conditions and Results of PC/DOP/C60 (89/10/1, wt/wt/wt) Composite Samples Crystallized at 200 MPa, Different Temperature for 6 h

Sample	Crystallization conditions (°C)	T_m (°C)	ΔH_m (J/g)
A1	220	220.94	4.392
A2	240	223.11	20.46
A3	260	235.46	32.70
A4	280	224.93, 244.91	23.28
A5	300	224.74, 249.21, 288.25	21.34

Table III. The Crystallization Conditions and Results of PC/DOP/C60 (89/10/1, wt/wt/wt) Composite Samples Crystallized at Different Pressure, 300°C for 6 h

Sample	Crystallization conditions (MPa)	T_m (°C)	ΔH_m (J/g)
A5	200	224.74, 249.21, 288.25	21.34
B1	300	238.73, 280.45	37.95
B2	400	225.92, 271.07	20.21
B3	500	227.66, 253.82	5.415

RESULTS AND DISCUSSION

C60 Dispersion in PC/C60 and PC/DOP/C60 Composites Disclosed by TEM

The dispersion state of a nanofiller in a polymer matrix is crucial to the physical properties of the corresponding composites. Figure 2 shows the TEM results of the as-prepared PC/C60 composite samples before the introduction of DOP. As can be seen, an overall good dispersion of C60 nanoaggregations in PC matrix was achieved, though the average size of the C60 agglomerations increased with the increase of C60 loading levels. Particularly, more uniform distribution of C60 aggregations was observed in a PC/C60 composite with 1.0 wt % C60 loading [Figure 2b]. The following DSC results (Table I) showed that such starting PC/C60 composites, with 0.5 and 1.0 wt % C60 loadings, respectively, were all amorphous. Thus it can be concluded at this point that the well dispersion of the C60 aggregations in PC matrix has not been influenced by the crystal formation of the polymer.

The results of further morphological investigation indicated that the average size of C60 agglomerations, as well as their morphologies, was affected to certain extent after the DOP incorporation (Figure 3). However, they still attained a relative satisfactory dispersion state in nanoscale [Figure 3(a)]. This suggested that the adopted physical and mechanical route, i.e. premixing at high speed followed by melt compounding, was a promising method in the successful fabrication of PC/DOP/C60 ternary

Table IV. The Crystallization Conditions and Results of PC/DOP/C60 (89/10/1, wt/wt/wt) Composite Samples Crystallized at 300 MPa, 300°C for Different Time

Sample	Crystallization conditions (h)	T_m (°C)	ΔH_m (J/g)
C1	4	231.58	28.99
B1	6	238.73, 280.45	37.95
C2	9	245.43, 280.27	45.44
C3	12	237.45, 274.79	43.68
C4	24	263.00	55.49

Table V. The Crystallization Conditions and Results of PC/DOP/C60 Composite Samples with Different Composition Crystallized at 300 MPa, 300°C for 6 h

Sample	Composition (PC/DOP/C60, wt/wt/wt)	T_m (°C)	ΔH_m (J/g)	X_c (%)
D1	89.5/10/0.5	236.66, 271.89	44.17	44.99
D2	79.5/20/0.5	235.43	44.35	50.85
B1	89/10/1	238.73, 280.45	37.95	38.87
D3	79/20/1	234.79	44.47	51.31

composites. The typical morphologies of C60 aggregations, observed by high resolution TEM, were also shown in Figure 3(b,c) for reference.

The literature already identified several techniques to blend fullerene with polymers.[33] Physical mixing by utilizing organic solvents, one of the simplest techniques, had difficulty in complete removal of the used solvents, and caused environmental problems. Surface functionalization of fullerenes may promote their dispersion in a polymer matrix. However, they lost certain precious properties of original fullerenes. So the above TEM results showed that well-dispersed PC/C60 and PC/DOP/C60 composites were fabricated respectively by an easy physical and mechanical route, i.e., premixing at high speed followed by melt compounding.

WAXD Results

WAXD was employed to determine the crystal form of the PC crystals obtained in the high-pressure crystallized PC/DOP/C60 blend samples. Figure 4 gives out the WAXD pattern of a PC/DOP/C60 (89/10/1, wt/wt/wt) composite sample, crystallized at 300 MPa, 300°C for 24 h, which is typical of the obtained profiles for such characterization. All main diffraction lines should be assigned to monoclinic form, just as those of PC or PC/DOP samples crystallized at high pressure.[30,34] The relative intensity of the corresponding peaks was somewhat different for various prepared samples. Nevertheless, the positions of the main diffraction lines remained almost the same. This indicated that no new crystal form of the polymer was crystallized in the presence of C60 at high pressure.

Thermal Analysis

Starting PC/C60 and PC/DOP/C60 Composites. Figure 5 and Table I show the DSC results of the as-fabricated starting PC/C60 and PC/DOP/C60 composites with different composition. The DSC measurements revealed that both PC/C60 samples (PC1 and 2) were amorphous, with the value of glass transition temperature more or less the same. The DSC also showed that samples PC3 and 5, both incorporated with 10 wt % DOP, were amorphous, and the glass transition temperature T_g increased with the increase of C60 loadings. However, compared with that of the original PC (T_g: 147.20°C), their glass transition temperatures were still decreased significantly by the introduction of the plasticizer. The decrease of the glass transition temperature indicated the increase of the free volume of the amorphous regions for the polymer. This allowed the rearranging of the rigid polymer chains into a more energetically favored state to hasten crystal growth during the following experiments.

When the compounding ratio of DOP was increased to 20 wt %, both samples PC 4 and 6, with 0.5 and 1.0 wt % C60 loadings, respectively, were crystallized just during the 15 min melt blending process. The melting points were more or less the same, and the melting enthalpy increased with the increase of C60 loadings. Particularly, for sample PC 6, cold crystallization occurred at 138.30°C during the heating scan of DSC. The previous studies on PC/DOP blends showed that only amorphous material was obtained after the melt compounding of 80 wt % PC with 20 wt % DOP.[30] So this indicated that C60 played an important role in the hastening of the crystallization of the polymer.

Effect of Temperature. The PC/DOP/C60 (89/10/1, wt/wt/wt) composite was selected for the high pressure experiments by varying temperature, pressure, and crystallization time. Figure 6 and Table II show the DSC results of the blend samples

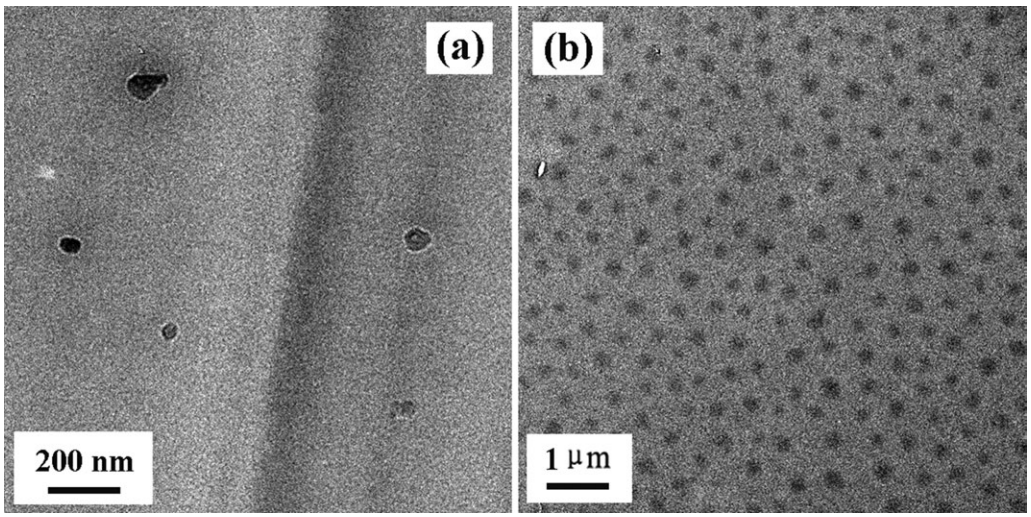

Figure 2. TEM photographs of the PC/C60 composite samples with 0.5 wt % (a) and 1.0 wt % (b) C60 loadings, respectively.

Applied Polymer SCIENCE

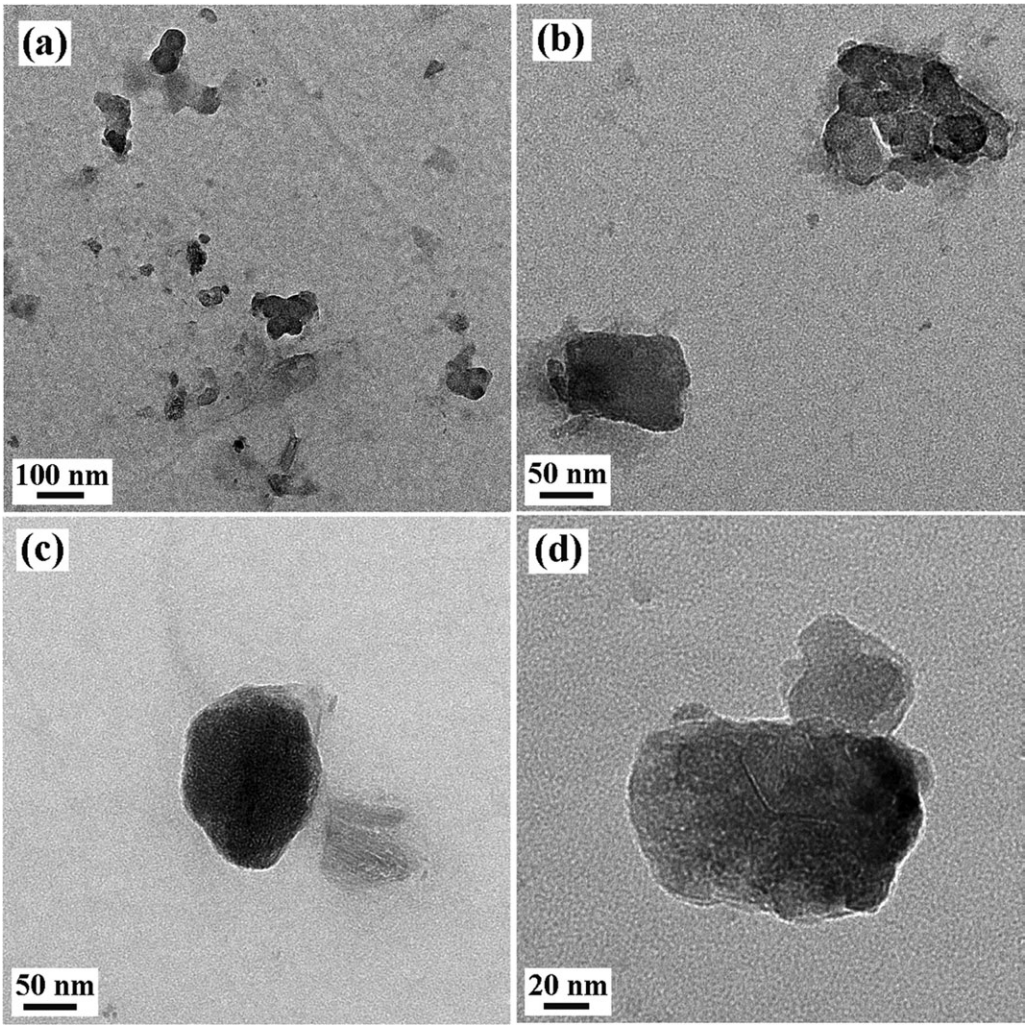

Figure 3. TEM photograph of the PC/DOP/C60 (89/10/1, wt/wt/wt) composite sample (a), and the typical morphologies of the C60 nanoaggregations in the polymer matrix (b–d) revealed by high resolution TEM.

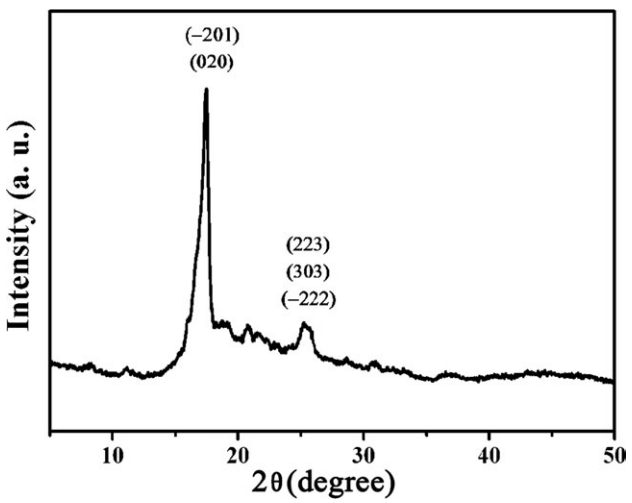

Figure 4. The WAXD pattern of PC/DOP/C60 (89/10/1, wt/wt/wt) composite sample C4 crystallized at 300 MPa, 300°C for 24 h.

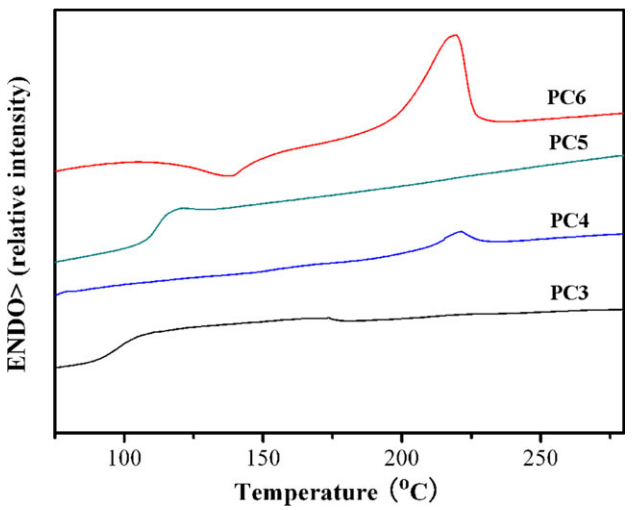

Figure 5. DSC curves of the starting PC/DOP/C60 composite materials. [Color figure can be viewed in the online issue, which is available at wileyonlinelibrary.com.]

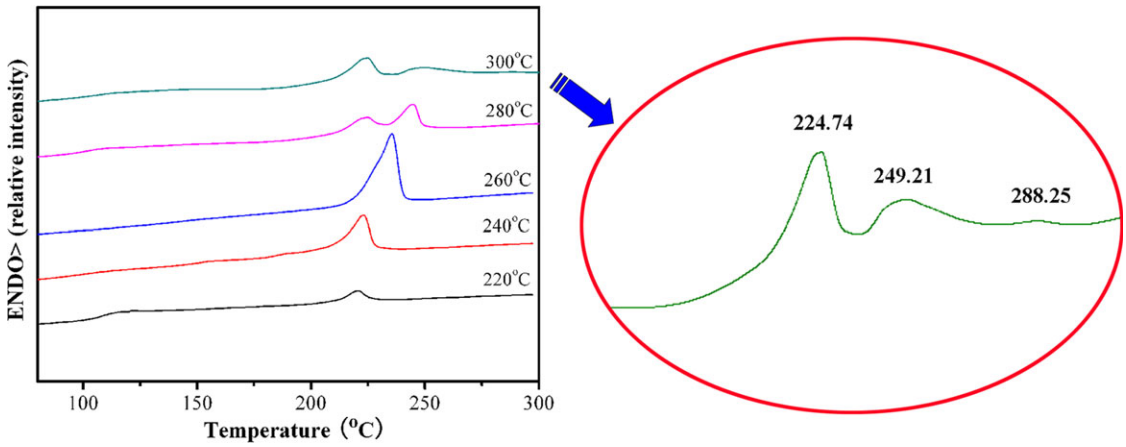

Figure 6. Left: DSC curves of PC/DOP/C60 (89/10/1, wt/wt/wt) composite samples crystallized at 200 MPa, different temperature for 6 h. Right: the magnified view of the DSC profile for the sample A5 crystallized at 300°C. [Color figure can be viewed in the online issue, which is available at wileyonlinelibrary.com.]

crystallized at 200 MPa, different temperature for 6 h. The results revealed that both the melting point and melting enthalpy increased with the increase of crystallization temperature during 220–260°C. When the crystallization temperature was increased to 280°C, two melting points were detected. The low and high endothermic regions should associate with the melting of two distinct populations of crystals, which resulted from primary crystallization and secondary crystallization, and were both present in the as-crystallized material.[30] Three peaks emerged on the DSC curve of the sample crystallized at 300°C. The positions of the two peaks at low-temperature side were consistent with those of the sample crystallized at 280°C. Although the intensity of the peak at high-temperature side was relatively weak, the astonishing point was that it reached 288.25°C, which was around 40°C higher than that of the samples crystallized at normal pressure.[30] Previous studies showed that pressure-treatment on PC/DOP blends could only obtain samples with melting points within the range of 152.78–247.19°C.[30] A PC sample with the melting point of 288.71°C was once prepared by bulk crystallization at high pressure.[34] Nevertheless, it was crystallized for 10 days, and the endowed melting enthalpy was 1.88 J/g.[34] Thus, the relative fast growth of the polymer crystals with a high melting point should be attributed the introduction of C60. The melting enthalpy began to decrease when the crystallization temperature was above 280°C. This was partly due to the high-temperature degradation of the previously formed PC crystals in the samples.

Effect of Pressure. Figure 7 and Table III give out the DSC results of the PC/DOP/C60 (89/10/1, wt/wt/wt) blend samples crystallized at different pressure, 300°C for 6 h. It was showed that two melting endotherms emerged on the DSC curves when the pressure was increased above 300 MPa. With the increase of the applied pressure, the low-temperature melting points decreased, and then remained more or less the same. Although the high-temperature melting points showed a decreasing tendency, they were still higher than those of the high-pressure crystallized PC/DOP samples.[30] The sample crystallized at 300 MPa attained the maximum value of melting enthalpy in this group samples. Nevertheless, the melting enthalpy decreased with the pressure further increased. The increase of supercooling, along with the increase of pressure, inhabited the diffusion rate of the PC molecular chains, and reduced the growth rate of the polymer crystals.[35] The DSC data on the sample crystallized at 300 MPa, 300°C for 6 h (melting points: 238.73 and 280.45°C; melting enthalpy: 37.95 J/g), suggested that, under appropriate experimental conditions, and by the introduction of DOP and C60, the crystal growth rate and crystal perfection of the polymer were improved simultaneously.

Effect of Crystallization Time. Figure 8 and Table IV show the DSC results of the PC/DOP/C60 (89/10/1, wt/wt/wt) composite samples crystallized at 300 MPa, 300°C for different time. Only one melting temperature was detected by DSC for the sample crystallized for 4 h. Apart from the main endotherms, weak peaks emerged on the high-temperature sides of the DSC curves

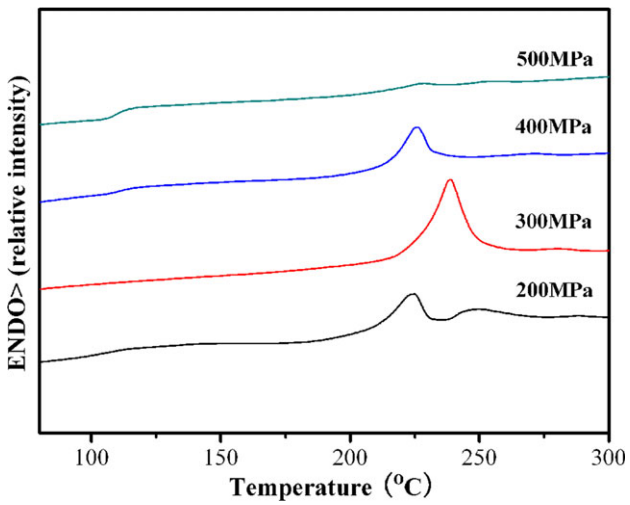

Figure 7. DSC curves of PC/DOP/C60 (89/10/1, wt/wt/wt) composite samples crystallized at different pressure, 300°C for 6 h. [Color figure can be viewed in the online issue, which is available at wileyonlinelibrary.com.]

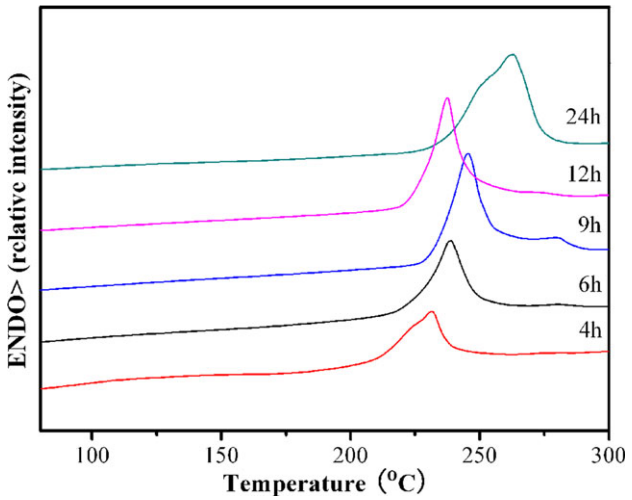

Figure 8. DSC curves of PC/DOP/C60 (89/10/1, wt/wt/wt) composite samples crystallized at 300 MPa, 300°C for different time. [Color figure can be viewed in the online issue, which is available at wileyonlinelibrary.com.]

of the sample crystallized for 6, 9, and 12 h. For these three samples, the melting points of the main peaks at low-temperature sides increased and then decreased with the increase of crystallization time. However, the high-temperature peaks gradually shifted to the low-temperature peaks. More attention should be paid to the sample crystallized for 24 h. The melting point of its main peak, with a shoulder at low-temperature side, reached 263.00°C, which was almost 32°C higher than that of the sample crystallized for 4 h. Furthermore, the variation tendency of the melting enthalpy of the samples in this group was meaningful. With the crystallization time increased during 4–9 h, the melting enthalpy increased all the time. And then, it decreased, as shown by the DSC data for the sample crystallized for 12 h. However, the melting enthalpy increased once again when the crystallization time was further increased. DSC revealed that the melting enthalpy of the sample crystallized for 24 h attained the value of 55.49 J/g, which was around twice that of the sample crystallized for just 4 h. The thermal analysis results for the samples in this group, crystallized at constant temperature and pressure for different time, indicated that there might be a competition between crystallization and high-temperature degradation, during the polymer crystallization in the ternary blend at high pressure. By controlling such competition process, a fully-crystallized PC/DOP/C60 composite with a high melting point, can be finally obtained, as reflected by the DSC data of the sample crystallized for 24 h. This may enlarge its application areas as a heat-resistant material.

Effect of Composition. Figure 9 and Table V show the DSC results of PC/DOP/C60 composite samples with different composition, crystallized at 300 MPa, 300°C for 6 h. Two melting points were detected for both the samples incorporated with 10 wt % DOP. With the increase of C60 loading level, the value of their main endotherms and weak peaks, at low and high temperature sides, respectively, increased as well. However, the crystallinity of PC decreased. The high-pressure experimental results on PC/DOP/C60 ternary blends with 10 wt % DOP incorporation agreed well with the conclusions by Yang et al. on molecular dynamics simulation.[36] This was somewhat different from that of the starting materials. It seems that the role of C60 at high pressure was in promoting the formation of polymer crystals with a higher melting point, in the ternary blends with relative low DOP concentration. When the incorporation ratio of DOP was increased to 20 wt %, only single endotherms were observed on the DSC curves of corresponding high-pressure crystallized samples. With the C60 loading increased, the melting points, as well as the crystallinity, remained more or less the same, as shown by the DSC data of the samples D2 and 3. It can also be noted form this group samples that the crystallinity increased, and the melting points of the main peaks slightly decreased, with DOP concentration increased and C60 loading remained the same.

SEM Observation on the Controllable Growth of Crystalline Polymeric Structures

Figure 10(a) shows the secondary electron image of the etched fracture surface of the PC/DOP/C60 (89/10/1, wt/wt/wt) composite sample crystallized at 200 MPa, 220°C for 6 h. As can be seen, zero-dimensional nanogranules with smooth surfaces, ranging in size from dozens to hundreds of nanometers, were crystallized under relatively large supercooling. The granules were observed after the applied etching process. Therefore, they were single crystalline. With the increase of crystallization temperature, more one-dimensional (1D) lamellar crystallites were observed [Figure 10(b)], which were apparently transformed from the nanogranules by a merging process. Two-dimensional (2D) snowflake-shaped dendrites appeared in the sample crystallized at still higher temperature, i.e. 300°C [Figure 10(c)]. However, a zoom-in view on such dendrites indicated that they were still evolved from the merged granules [Figure 10(d)].

Other conditions being the same, another sample was crystallized at 200 MPa, 300°C for 12 h. DSC data showed that only single endotherm was detected by the heating scan. The melting

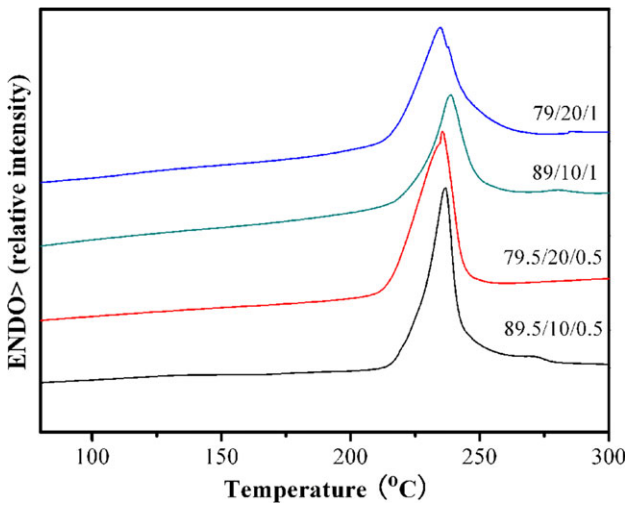

Figure 9. DSC curves of PC/DOP/C60 (89/10/1, wt/wt/wt) composite samples crystallized at different pressure, 300°C for 6 h. [Color figure can be viewed in the online issue, which is available at wileyonlinelibrary.com.]

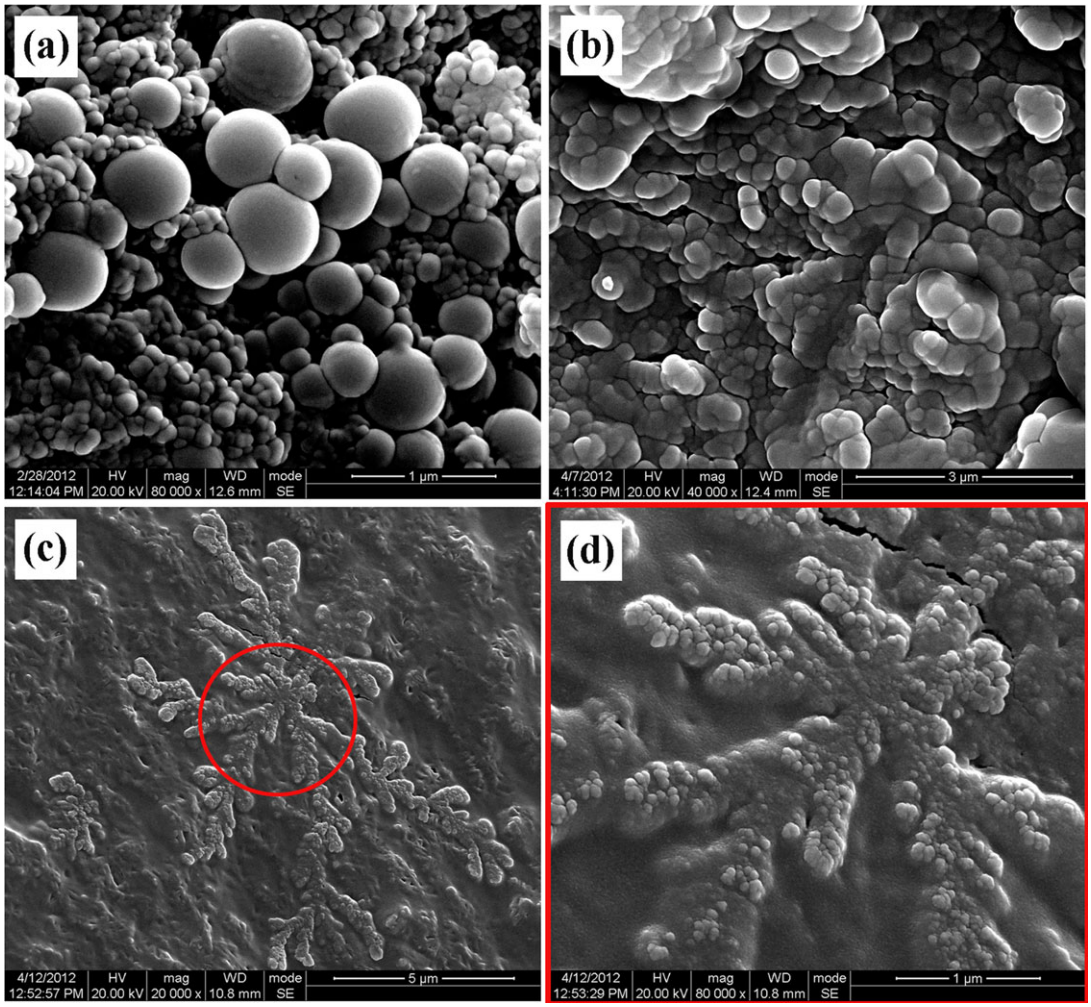

Figure 10. Secondary electron images of PC/DOP/C60 (89/10/1, wt/wt/wt) composite samples, crystallized at 200 MPa, different temperature for 6 h: (a) 220°C; (b) 280°C; (c, d): 300°C. (d) is the magnified view of the portion highlighted by an elliptical frame in (c). [Color figure can be viewed in the online issue, which is available at wileyonlinelibrary.com.]

point and melting enthalpy were 255.05°C and 44.27 J/g, respectively. The typical secondary electron image of the sample was shown in Figure 11(a), in which three-dimensional (3D) crystalline spiked spheres were observed. The branching crystals of the spiky spheres nucleated at their centers, and did not branching again along the radial directions [Figure 11(b,c)]. Morphological observations suggested that such 3D polymer spheres began with the nanogranules, and then developed by merging process through the stages of 1D lamellar crystallites and 2D dendrites, due to the synergistic action of C60 and DOP. We also noted that dense dendritical network was formed in the sample [Figure 11(d)]. Just as that in a high-pressure crystallized PC/DOP blend, this should be ascribed to the bulk crystallization of the polymer induced by DOP only.[30]

Figure 12 shows the secondary electron images of PC/DOP/C60 (89/10/1, wt/wt/wt) composite sample, crystallized at 300 MPa, 300°C for 6 h. With the increase of pressure, no 2D dendritic crystal was observed. However, the nanogranules merged into another 2D form, plate crystals, as shown in Figure 12(a). And then, the 2D platelets organized into 3D micro-spheres with rugged surfaces [Figure 12(b,c)]. Ordinary spherulitic structures of the polymer were also formed in this sample [Figure 12(d)], due to the DOP-induced bulk crystallization at high pressure.[30] When the spherulites developed from their initial fiber stage and grew mature, they impinged with one another during the growth process and became polyhedral. The co-existence of the rugged crystalline spheres and the normal spherulites further confirmed the co-existence of two crystallization regions in one sample. The rugged spheres were crystallized by the cooperation of C60 and DOP, while the formation of the normal spherulites was promoted by DOP alone.

With the applied pressure further increased, 3D micro-spheres with another form were crystallized. Figure 13 gives out the secondary electron image of PC/DOP/C60 (89/10/1, wt/wt/wt) composite sample, crystallized at 500 MPa, 300°C for 6 h. Interestingly, isolated porous spheres that presented a homogeneous morphology were observed after the etching process. Microspheres with porous structures were also obtained through high pressure bulk crystallization of single component PC by a double-heat treatment.[34] However, it took 10 days to crystallize the

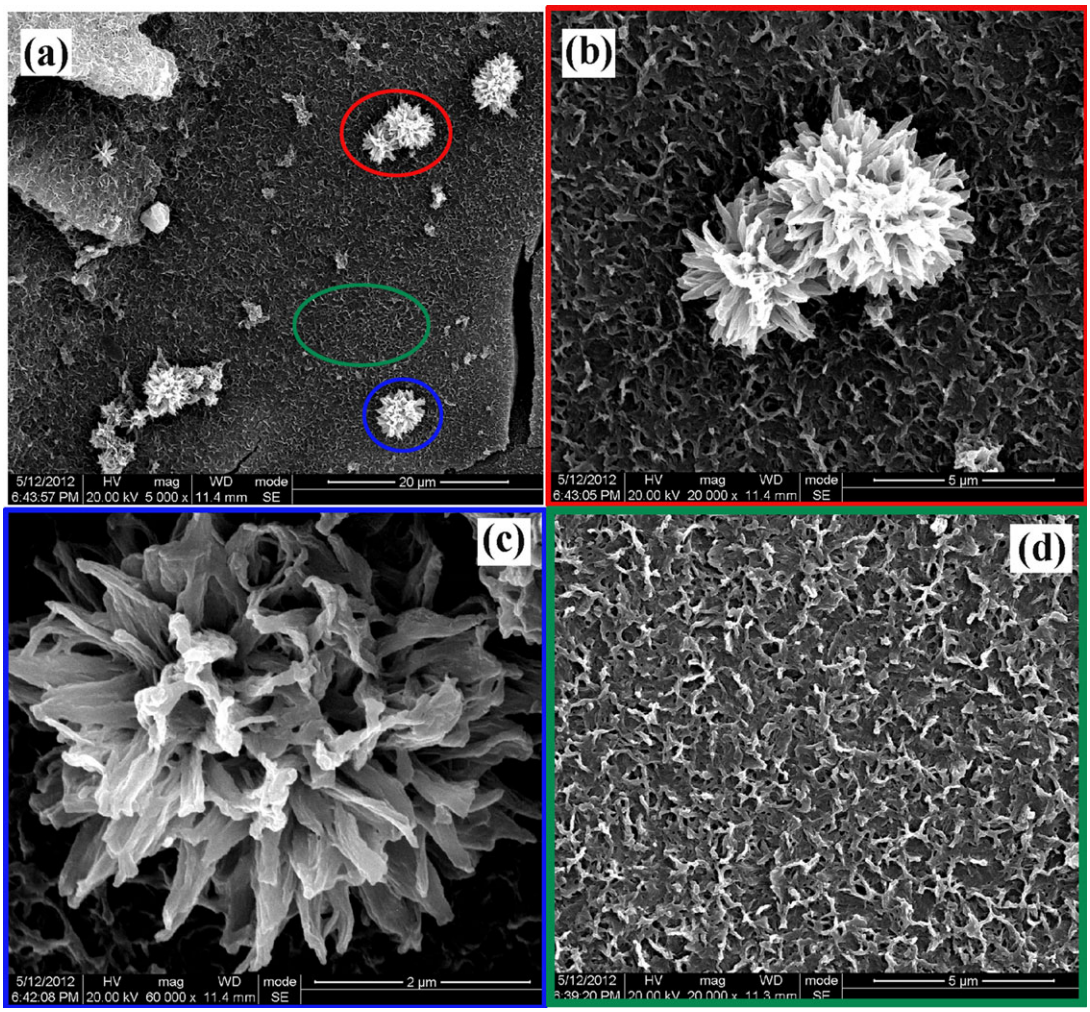

Figure 11. Secondary electron images of PC/DOP/C60 (89/10/1, wt/wt/wt) composite sample, crystallized at 200 MPa, 300°C for 12 h. (b), (c), and (d) are the magnified views of the portions highlighted by elliptical frames in (a), respectively. [Color figure can be viewed in the online issue, which is available at wileyonlinelibrary.com.]

sample. No similar micro-sphere was observed in the previously high-pressure crystallized PC/DOP blend samples. Furthermore, WAXD and DSC revealed that the PC/C60 composite samples crystallized at high pressure for 6 h were all amorphous. So the fast crystallization of the 3D micro-spheres with porous structures should also be attributed to the coeffect of DOP and C60 in the ternary blends.

Figure 14 shows the secondary electron images of PC/DOP/C60 (89/10/1, wt/wt/wt) composite sample, crystallized at 300 MPa, 300°C for 9 h. In addition to the above-described morphologies for the sample crystallized at the same pressure and temperature for 6 h, a crystalline globule in nanoscale, consisting of still smaller nanogranules, was observed. The formation of the rugged globules was due to the recrystallization of the polymer in the ternary blends.[37] This is also confirmed by the fact that more such globules were revealed in a high-pressure crystallized PC/DOP/C60 sample in which the C60 loading level was substantially decreased.

Peony-like stereo-open spherulitic structures were crystallized by changing the composite composition. The secondary electron images of the fracture surface of a PC/DOP/C60 (89.5/10/0.5, wt/wt/wt) composite sample, crystallized at 300 MPa, 300°C for 6 h, were shown in Figure 15. It can be observed that the crystalline peonies were flourishing in the ternary blends [Figure 15(a)]. Their wide and thin leaves densely branched along the radial direction, and formed a unique nanostructured micrometer-sized crystalline entity of the polymer [Figure 15(b)]. The growth of such peony-like spherulitic structures was attributed to the decreased loading level of C60, which decreased the number of nucleating centers, and then allowed the relatively full propagation of the crystal fibrils from a given C60-nucleated spot, with the help of DOP, of course.

The controllable growth of the unique 3D crystalline polymeric structures, including the micrometer-sized spiky, rugged and porous spheres, and the peony-like stereo-open enetities, together with the nanoscale globules with rugged surfaces, may give some interesting suggestions for the design of new functional materials. As can be seen, the crystalline structures can be easily exposed and isolated with the applied selective etching

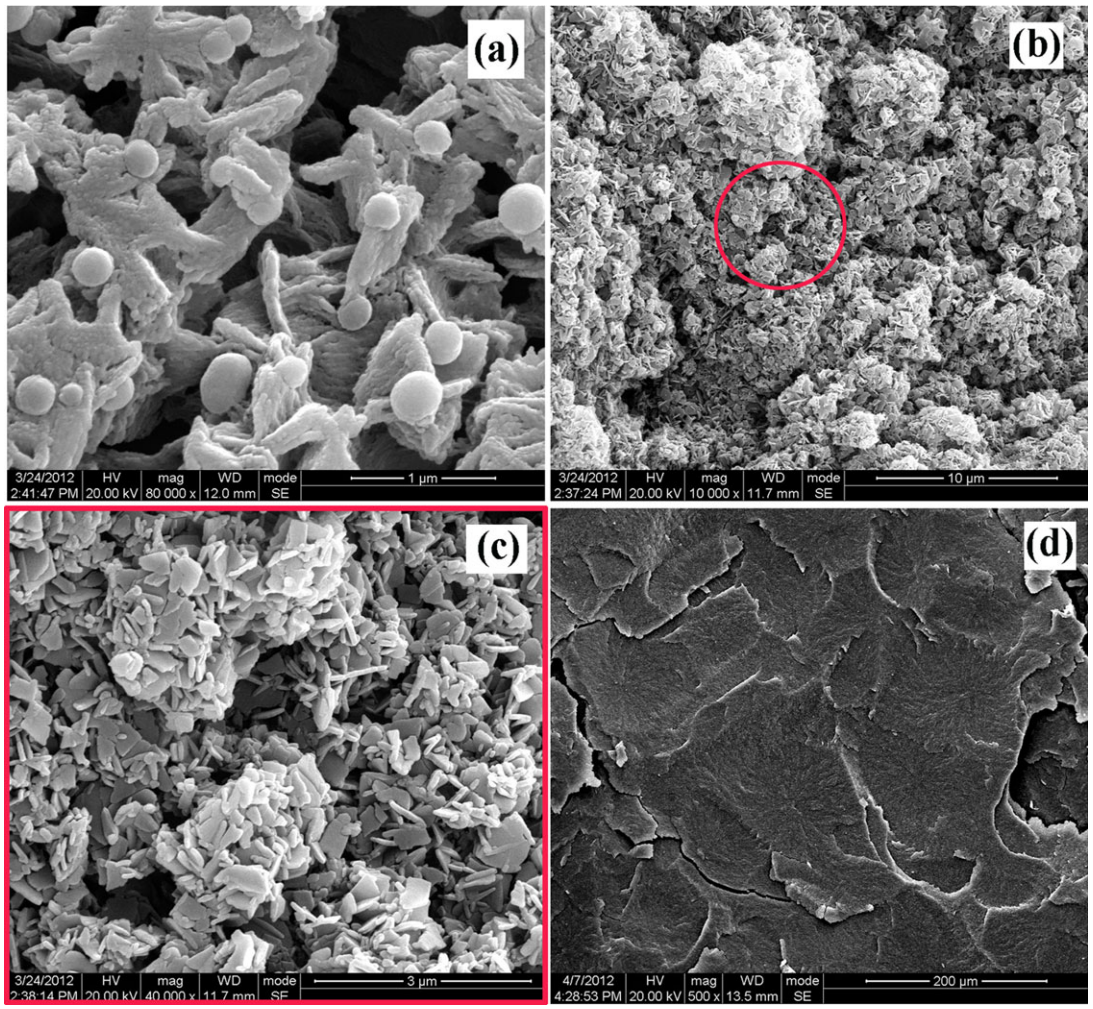

Figure 12. Secondary electron images of PC/DOP/C60 (89/10/1, wt/wt/wt) composite sample, crystallized at 300 MPa, 300°C for 6 h. (c) is the magnified view of the portion highlighted by an elliptical frame in (b). [Color figure can be viewed in the online issue, which is available at wileyonlinelibrary.com.]

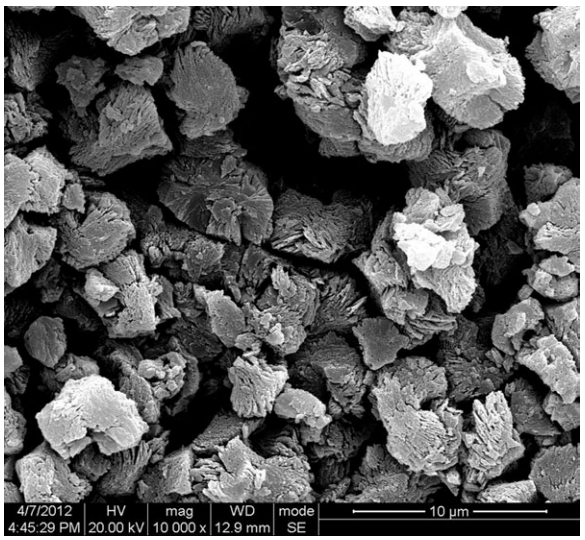

Figure 13. Secondary electron image of PC/DOP/C60 (89/10/1, wt/wt/wt) composite sample, crystallized at 500 MPa, 300°C for 6 h.

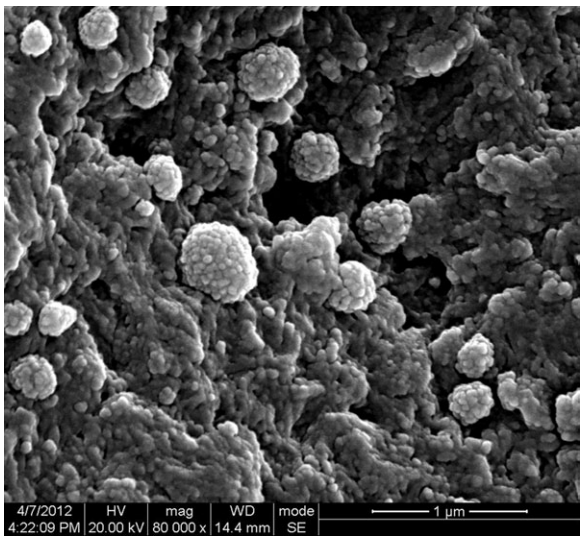

Figure 14. Secondary electron image of PC/DOP/C60 (89/10/1, wt/wt/wt) composite sample, crystallized at 300 MPa, 300°C for 9 h.

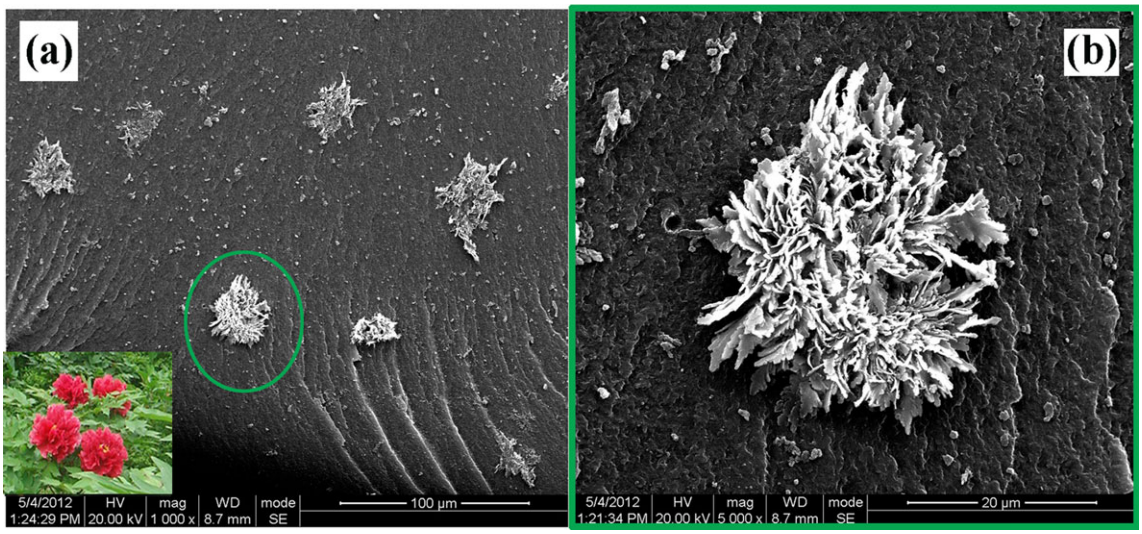

Figure 15. Secondary electron images of PC/DOP/C60 (89.5/10/0.5, wt/wt/wt) composite sample, crystallized at 300 MPa, 300°C for 6 h. The inset in (a) is a photograph of peonies, and (b) is the magnified view of the portion highlighted by an elliptical frame in (a). [Color figure can be viewed in the online issue, which is available at wileyonlinelibrary.com.]

technique, and their tunable surface structures allow the loading and controllable release of a variety of guest molecules. With the crystalline morphology and surface properties precisely manipulated, combined with the excellent thermal and mechanical properties of the base polymer, the as-prepared polymeric structures may pursue niche advanced applications in fillers, carriers, adsorbents, and so on.[38–40]

CONCLUSIONS

In summary, controllable fast growth of the crystalline structures of PC was achieved through the high-pressure crystallization of well-dispersed PC/DOP/C60 ternary nanocomposites, which were fabricated by an easy and solvent-free approach. Unique single-crystalline 3D structures, including micrometer-sized spiky, rugged and porous spheres, and peony-like stereo-open enetities, together with nanoscale globules with rugged surfaces, were crystallized by varying crystallization temperature, pressure, time, and composite composition. The 3D structures began with a nanogranule, and then developed by a merging process through the stages of respective 1D and 2D aggregations with different characteristics. With their crystalline morphology and surface properties precisely manipulated, the as-crystallized 3D polymeric structures may pursue niche advanced functional applications as surface active materials. In addition to the formation of the unique crystalline structures, the introduction of DOP and C60 into PC may change the mechanical properties of the original material, such as toughness. This will be further researched and then addressed in a follow up article.

ACKNOWLEDGMENTS

This work was supported by the National Natural Science Foundation of China (No. 50973089), and the Fundamental Research Funds for the Central Universities (No. SWJTU11CX056 and SWJTU11ZT10).

REFERENCES

1. Giacalone, F.; Martín, N. *Adv. Mater.* **2010**, *22*, 4220.
2. Sariciftci, N. S.; Smilowitz, L.; Heeger, A. J.; Wudl, F. *Science* **1992**, *258*, 1474.
3. Lu, G.; Li, L.; Yang, X. *Small* **2008**, *5*, 601.
4. Rajagopalan, M.; Oh, I. K. *ACS Nano* **2011**, *5*, 2248.
5. Langhe, D. S.; Hiltner, A.; Baer, E. *J. Appl. Polym. Sci.* **2012**, *125*, 2110.
6. Matsuda, Y.; Hanamura, R.; Takemura, Y.; Sugita, A.; Tasaka, S. *J. Appl. Polym. Sci.* **2012**, *126*, E116–E122.
7. Hasell, T.; Lagonigro, L.; Peacock, A. C.; Yoda, S.; Brown, P. D.; Sazio, P. J. A.; Howdle, S. M. *Adv. Funct. Mater.* **2008**, *18*, 1265.
8. Scardaci, V.; Sun, Z. P.; Wang, F.; Rozhin, A. G.; Hasan, T.; Hennrich, F.; White, I. H.; Milne, W. I.; Ferrari, A. C. *Adv. Mater.* **2008**, *20*, 4040.
9. Erben, C.; Boden, E. P.; Longley, K. L.; Shi, X. L.; Lawrence, B. L. *Adv. Funct. Mater.* **2007**, *17*, 2659.
10. Tang, B. Z.; Peng, H.; Leung, S. M.; Au, C. F.; Poon, W. H.; Chen, H. L.; Wu, X. Z.; Fok, M. W.; Yu, N. T.; Hiraoka, H.; Song, C. Y.; Fu, J. S.; Ge, W. K.; Wong, G. K. L.; Monde, T.; Nemoto, F.; Su, K. C. *Macromolecules* **1998**, *31*, 103.
11. Li, F. Y.; Li, Y. L.; Ge, Z. X.; Zhu, D. B.; Song, Y. L.; Fang, G. Y. *J. Phys. Chem. Solids* **2000**, *61*, 1101.
12. Wu, H. X.; Li, F.; Lin, Y. H.; Cai, R. F.; Tong, R.; Qian, S. X. *Polym. Eng. Sci.* **2006**, *46*, 399.
13. van Bavel, S.; Veenstra, S.; Loos, J. *Macromol. Rapid. Commun.* **2010**, 31, 1835.
14. Tsao, H. N.; Mullen, K. *Chem. Soc. Rev.* **2010**, *39*, 2372.
15. Liu, X. L.; Huettner, S.; Rong, Z. X.; Sommer, M.; Friend, R. H. *Adv. Mater.* **2012**, *24*, 669.

16. Erb, T.; Zhokhavets, U.; Gobsch, G.; Raleva, S.; Stuehn, B.; Schilinsky, P.; Waldauf, C.; Brabec, C. *J. Adv. Funct. Mater.* **2005**, *15*, 1193.
17. Moulé, A. J.; Meerholz, K. *Adv. Mater.* **2008**, *20*, 240.
18. Honda, S.; Ohkita, H.; Benten, H.; Ito, S. *Adv. Energy Mater.* **2011**, *1*, 588.
19. Ji, G. D.; Xue, G.; Ma, J. L.; Dong, C. Y. *Polymer* **1996**, *37*, 3255.
20. Sohn, S.; Alizadeh, A.; Marand, H. *Polymer* **2000**, *45*, 8879.
21. Alizadeh, A.; Sohn, S.; Quinn, J.; Marand, H. *Macromolecules* **2001**, *34*, 4066.
22. Krause, B.; Villmow, T.; Boldt, R.; Mende, M.; Petzold, G.; Pötschke, P. *Compos. Sci. Technol.* **2011**, *71*, 1145.
23. Lin, D. M.; Boschetti-de-Fierro, A.; Alexandre, M.; Abetz, C.; Böttcher, H.; Abetz, V.; Urbanczyk, L.; Jérôme, C.; Han, C. C. *Compos. Sci. Technol.* **2011**, 71, 1893.
24. Münstedt, H. *Polymer* **2011**, *52*, 3677.
25. Edwards, B. C. and Phillips, P. J. *Polymer* **1974**, *15*, 491.
26. Kyotani, M.; Kanetsuna, H. *J. Polym. Sci. Polym. Phys. Ed.* **1974**, *12*, 2331.
27. Gallez, F.; Legras, R.; Mercier, J. P. *J. Polym. Sci. Polym. Phys. Ed.* **1976**, *14*, 1367.
28. Legras, R.; Mercier, J. P.; Nield, E. *Nature* **1983**, *304*, 432.
29. Legras, R.; Bailly, C.; Daumerie, M.; Dekoninck, J. M.; Mercier, J. P.; Zchyi, M. V.; Nield, E. *Polymer* **1984**, *25*, 835.
30. Lu, J.; Huang, R.; Oh, I. K. *J. Polym. Sci. Pol. Phys.* **2007**, *45*, 2715.
31. Xi, D. K.; Huang, W. J.; Li, Z. P.; Lu, J.; Chen, X. L.; Zhou, Z. W. *Mater. Lett.* **2012**, *81*, 189.
32. Heiss, H. L. *Poly. Eng. Sci.* **1979**, *19*, 625.
33. Giacalone, F.; Martin, N. *Chem. Rev.* **2006**, *106*, 5136.
34. Lu, J.; Xi, D. K.; Huang, R.; Li, L. B. *J. Macromol. Sci. B* **2011**, *50*, 1018.
35. Hiramatsu, N.; Hirakawa, S. *Polym. J.* **1980**, *12*, 105.
36. Yang, H.; Zhao, X. J.; Li. Z. S.; Yan, F. D. *J. Chem. Phys.* **2009**, *130*, 074902.
37. An, N. L.; Liu, H. Z.; Ding, Y. C.; Lu, B. H.; Zhang, M. *Appl. Surf. Sci.* **2012**, *258*, 5052.
38. Vallet-Regi, M.; Balas, F.; Arcos, D. *Angew. Chem. Int. Ed.* **2007**, *46*, 7548.
39. Lu, J.; Tian, J. J.; Zhang, D. P.; Xi, D. K.; Huang, R. *Amino Acids* **2011**, *41*, S31.
40. Abe, S.; Tsujimoto, M.; Yoneda, K.; Ohba, M.; Hikage, T.; Takano, M.; Kitagawa, S.; Ueno, T. *Small* **2012**, *8*, 1314.